Cancer Nanotechnology

RESEARCH Open Access

Hyaluronan self-agglomerating nanoparticles for non-small cell lung cancer targeting

Joo-Eun Kim[1] and Young-Joon Park[2*]

*Correspondence:
parkyj64@gmail.com
[2] College of Pharmacy, Ajou University, Suwon City 443-749, Korea
Full list of author information is available at the end of the article

Abstract

Background: Owing to the limited amount of research, there are no nanoparticle-based anticancer agents that use hydrophilic drugs. Therefore, we developed irinotecan-loaded self-agglomerating hyaluronan nanoparticles (ISHNs). While irinotecan has high hydrophilicity, the resulting nanoparticle should possess high anticancer drug-loading capacity and allow selective targeting of the cluster of differentiation 44 (CD44) protein, which is overexpressed on the surface of tumor cells.

Results: The ISHNs were successfully made with hyaluronan (HA) as a targeting moiety, $FeCl_3$ as a binder, and D-glutamic acid (GA) as a stabilizer. The ISHNs self-agglomerated via chelating bonding and were lyophilized using a freeze dryer. The particle diameter and zeta potential of the ISHNs were 93.8 ± 4.48 nm and -36.3 ± 0.28 mV, respectively; a relatively narrow size distribution was observed. The drug fixation yield and drug-loading concentration were 58.3% and 1.75 mg/mL, respectively. Affinity studies revealed a tenfold stronger targeting to H23 ($CD44^+$) non-small-cell lung cancer (NSCLC) cells, than of A549 ($CD44^-$) cells.

Conclusion: We developed irinotecan-loaded ISHNs, which comprised irinotecan hydrochloride as a water-soluble anticancer agent, HA as a targeting moiety, $FeCl_3$ as a binder for self-agglomeration, and GA as a stabilizer; HA is a binding material for CD44 in NSCLC cells. Owing to their ease of manufacture, excellent stability, non-cell toxicity and CD44-targeting ability, ISHNs are potential nanocarriers for passive and active tumor targeting.

Keywords: Nanoparticle, Targeting, Hyaluronan, Irinotecan, Stability, NSCLC

Background

Despite the development of many anticancer drugs, efficient chemotherapy has not been achieved as there is no targeted drug delivery systems that can efficiently deliver chemotherapeutic drugs to cancer cells (Cho and Park 2010). Currently, the most widely used anticancer-drug delivery system is the injection of an intravenous infusion of the drug, which is dissolved in an organic solvent or into a surfactant for an insoluble or poorly soluble anticancer drug (Cho and Park 2014). These drug delivery systems are known to cause side effects when anticancer drugs are administered to normal cells rather than

cancer cells. Further, the organic solvents that are often used as excipients for anticancer drugs may cause toxic side effects, or the surfactants in anticancer drug formulations may necessitate pretreatment, such as the administration of strong steroids, owing to hypersensitivity (Liebmann et al. 1993). To overcome such limitations, a variety of tumor targeting methods, including passive or active targeting using nanotechnology or nanoparticle technology, have been studied (Park et al. 2017). These methods include the enhanced permeability and retention (EPR) effect for targeting moieties on the surface of the nanoparticles to enable high selectivity and specificity to tumor cells, and minimize the adverse effects in normal cells (Choi and Han 2018).

Nevertheless, research is limited to drug delivery systems that encapsulate only poor water-soluble drugs in nanoparticles (Kim et al. 2017). In the case of poor water-soluble anticancer drugs, it is easy to encapsulate drugs in various nanoparticles, such as poly lactic-co-glycolic acid (Son et al. 2017), micelles (Danafar et al. 2018), solid lipid nanoparticles (Gupta et al. 2017), liposomes (Seo et al. 2018), cyclodextrins (Jin et al. 2018), and nano-emulsions (Kim et al. 2017). These drug delivery nanoparticles employ the hydrophobic characteristics of drugs and offer great advantages as they are easy to research and develop, and show high stability in aqueous solutions for extended periods after synthesis (Kim et al. 2017).

The encapsulation of hydrophilic-anticancer drugs remains a technical challenge as their nature results in rapid dissolution and uncontrolled drug release in aqueous solution within a few hours, even if the drug is deep within the encapsulated structure (Kim et al. 2017; Kirtane et al. 2017; Sarisozen et al. 2017). Hence, research on water-soluble anticancer drug-loaded nanoparticles is limited and there has been no development of such therapeutic agents even though there is a high market demand for them. In this study, we aimed to develop self-agglomerating hyaluronan nanoparticles (SAHNs) with the capability of loading hydrophilic and water-soluble anticancer agents, and targeting tumor cells. To apply self-agglomerating nanoparticle technology, this study investigated the specific properties of irinotecan hydrochloride and hyaluronan (HA)—an endogenous substance and a naturally water-soluble carbohydrate that is found in the human body. A previously described chelating technique (Zhu et al. 2013) of the μ-oxo species was used, which is generated by the addition of trivalent iron ions, such as ferric chloride (Mercê et al. 2002).

HA was employed as a drug carrier for tumor targeting, owing to its specific binding to the cluster of differentiation 44 (CD44) receptor, which is overexpressed in tumor cells. HA is composed of repeating dimer units of N-acetyl-glucosamine and glucuronic acid, and it is a negatively charged linear polysaccharide. HA is widely distributed throughout the epithelial and neural tissues of the human body and has been investigated as a target molecule owing to its unique properties (Karbownik and Nowak 2013). HA only binds to CD44, which is a cell surface biomarker that is overexpressed in the tumor tissue. A novel strategy for active tumor targeting involves the specific binding of CD44 to HA in cancer therapy. Several nanocarrier formulations have been developed in which HA is connected to nanocarrier particles, such as HA-coated nanoparticles, HA nanogels, and HA-decorated nanoparticles (Liang et al. 2016, Mohtashamian and Boddohi 2017). These HA-nanocarriers have excellent targeting affinities for tumors, but their limited encapsulation of water-soluble drugs is a serious challenge.

Irinotecan, a water-soluble anticancer agent, inhibits DNA synthesis by interfering with the action of enzymes for DNA replication and transcription, which act on topoisomerase I inhibitors. Irinotecan is mainly used in the treatment of colorectal and lung cancers. The main side effects of irinotecan include problems with hematopoiesis, such as leukocyte depletion of approximately 80–90% and platelet reduction of 15–30%. To prevent hematopoiesis and the reduction of drug efficacy, we developed iron-ion-synthesized nanoparticles containing HA and irinotecan. To fabricate hyaluronan self-agglomerating nanoparticles for tumor targeting in the absence of organic solvents, chemical conjugates, and surfactants, we studied nanoparticles using trivalent transition metal ions. In particular, self-agglomerating nanoparticle formation technology using ionic bonds (Mercê et al. 2002) can be readily applied to mass production and used immediately in the pharmaceutical industry; thus, it is possible to specifically target drugs to cancer cells. Therefore, it is possible to improve the safety and efficacy of existing water-soluble anticancer drugs (e.g., increase in efficacy, decrease in side effects, and improvements in administration methods) and to continuously expand into the market.

This study describes the method of preparation, characterization of the prepared particles, and the cancer cell targeting ability of ISHNs encapsulating irinotecan, as a model water-soluble anticancer drug. Specifically, this study aimed to investigate specific strategies to load irinotecan, a model water-soluble anticancer agent, into ISHNs by studying the attachment of the nanoparticle core through electrostatic interaction, and the chelation method between the negatively charged carboxyl group of irinotecan and trivalent transition metal ions.

In summary, this study successfully developed the following: (1) hyaluronan self-agglomerating nanoparticles that could specifically bind to CD44 and target cancer cells, and (2) irinotecan self-agglomerated with HA.

Results and discussion

Preparation of SAHNs and ISHNs

To manufacture a nanoparticle-based anticancer agent containing a hydrophilic drug, which can target tumor cells without eliciting any side effects on normal cells, we developed nanoparticles for active–passive targeting in non-small-cell lung cancer (NSCLC). The pore cut-off size in the tumor vessels was 300 nm or less; however, to avoid the EPR effect and RES, it was necessary to make nanoparticles that were maintained below 150 nm.

In preliminary studies, it was confirmed that aggregation occurs through covalent bonding between hyaluronan and the dislocation metal, and through this, it was confirmed that it was possible to undertake research to develop a nanoparticle. (Mercê et al. 2002; Kim et al. 2017). However, if the molecular weight, concentration, and pH of hyaluronan were out of the appropriate range, the nanoparticles were not manufactured. Then, only various aggregation or precipitation phenomena were observed. Therefore, an experiment was needed to confirm the optimal ratio of hyaluronan and iron ions, in which nanoparticles could be formed through specific parameters. When the specific pH was exceeded, the particle size was increased to 300 nm or more, and when a high concentration of HA was used, the nanoparticle size became 400 nm or more. In addition, when high molecular weight HA was used, the particle size was as

Table 1 Physicochemical properties of SAHNs. The data are expressed as the mean ± standard deviation (SD, $n = 3$). Characterization of SAHNs by molecular weight of HA

Volume of 0.05 M Fe^{3+} ion (μL)	v/v (%)	800,000 Da	950,000 Da	1,500,000 Da	3,600,000 Da
150	0.0099	139 nm	130 nm	163 nm	N.D
200	0.0132	112 nm	108 nm	140 nm	N.D
250	0.0164	109 nm	120 nm	164 nm	95.2 nm
300	0.0196	125 nm	137 nm	151 nm	102 nm
350	0.0228	233 nm	282 nm	144 nm	117 nm

* *N.D* not detected: the results did not meet the criteria

Data are expressed as mean ± standard deviation (SD, $n = 3$)

A comparative study of molecular weight selection according to HA was performed at a concentration of 0.1% HA

Table 2 Characterization of SAHNs at different pH values

pH	Size (nm)	% SD	PDI	Zeta potential (mV)	Zeta potential SD (mV)
2.81	109	1.32	0.066	− 30.3	5.84
3.00	112	1.51	0.094	− 31.2	7.36
4.10	149	1.06	0.063	− 33.9	6.35
5.10	213	1.11	0.035	− 35.8	5.35
6.25	247	1.37	0.114	− 44.1	5.23
7.20	267	3.63	0.167	− 46.6	4.62

Data are expressed as mean ± standard deviation (SD, $n = 5$)

SD means standard deviation, PDI means polydispersity index

small as 150 nm or less, but it was unstable and could not be maintained for a long time. In addition, when the PDI value exceeded 0.2, the stability of the nanoparticles was not maintained. Also, when the concentration of L-glutamic acid, a stabilizer, was out of the range of 0.01 to 0.02 M, the size of the nanoparticles increased to 200 nm or more. The reason for performing the experiment with the specific parameters that are described in Tables 1, 2, 3, 5 was to determine the optimal ratio of hyaluronan and iron ions.

As shown in Table 1, to ascertain the size dependency on the molecular weight of HA, SAHNs were prepared using the methods described below. However, its methods changed only the molecular weight of HA from 800,000 Da to 3,600,000 Da. As shown in Table 1, the molecular weight of HA did not affect particle size. In further studies, changes in the particle size for the HA concentration occurred.

As shown in Table 2, the particle size change of SAHNs in different pH environments was observed. The rationale for performing this experiment is that the pH range in which cancer cells proliferate is known to be acidic. When the size of the cancer-targeting nanoparticles increased to 300 nm or more, the efficiency in vivo decreased for passive targeting due to the EPR effect or RES. However, even when exposed to an environment with high external pH, the particle size remained low

Table 3 Stoichiometric ratio of trivalent transition metallic ions and hyaluronan

Volume of 0.05 M Fe^{3+} ion (μL)	v/v (%)	Stoichiometric ratio (HA disaccharide: Fe^{3+})	Size (nm)	% SD	PDI	pH value
0.3% Hyaluronan and $FeCl_3$						
400	0.0260	1:0.17	542	–	0.416	2.58
420	0.0272	1:0.18	424	–	0.277	2.58
440	0.0285	1:0.19	492	–	0.352	2.57
460	0.0298	1:0.19	479	–	0.306	2.58
480	0.0310	1:0.20	428	–	0.236	2.58
500	0.0323	1:0.21	407	–	0.214	2.57
520	0.0335	1:0.22	392	–	0.217	2.57
0.1% Hyaluronan and $FeCl_3$						
140	0.0092	1:0.18	142	4.74	0.365	2.93
150	0.0099	1:0.19	130	7.58	0.208	2.92
160	0.0106	1:0.20	97.8	4.28	0.212	2.90
180	0.0119	1:0.23	88.5	3.20	0.176	2.88
200	0.0132	1:0.25	93.9	3.01	0.143	2.86
220	0.0145	1:0.28	101	1.98	0.128	2.84
240	0.0157	1:0.30	110	2.58	0.090	2.82
260	0.0170	1:0.33	120	1.87	0.157	2.80
280	0.0183	1:0.35	122	4.37	0.144	2.78
300	0.0196	1:0.38	137	1.86	0.127	2.77
310	0.0202	1:0.39	177	0.50	0.252	2.77
320	0.0209	1:0.40	233	1.52	0.262	2.76

SD standard deviation, *PDI* polydispersity index

Data are expressed as mean ± standard deviation (SD, $n = 5$)

(< 300 nm). From these results, it was estimated that passive targeting of NSCLC cells was possible because we aimed to keep the particle size less than 150 nm in an acidic environment of pH ranging from 2.8 to 4.1. SAHNs in an environment with a pH of 2.8 to 4.1 showed a low PDI value of less than 0.1 and a stable Zeta potential value of − 30 mV.

To investigate the effects of the variations in proportion on the preparation of SAHNs, ferric chloride, supplied as iron (III) ions, was added to 15 mL HA solution, and then experiments were conducted with constant stirring at 250 rpm at ambient temperature for 5 min. The methods changed only the stoichiometric ratio (HA disaccharide: iron (III) ions [$FeCl_3$]); the amount of added iron (III) ion to hyaluronan was adjusted from 1:0.17 to 1:0.40, and the results are shown in Table 3.

HA is a natural long-chain polymeric compound based on a disaccharide that is a combination of D-glucuronic acid and N-acetyl-D-glucosamine (Kogan et al. 2007). Each disaccharide, as a monomer, contains one carboxylic group that is engaged in a coordinate bond with iron(III) ions ($FeCl_3$), where the stoichiometric ratio indicates the proportion between the disaccharide and iron (III) ions (i.e., *reaction ratio*) (Mercê et al. 2002; Kim et al. 2017).

As shown in Table 3 (up), the particle size varied with the specific ratio of HA disaccharide: iron (III) ions [$FeCl_3$]. First, to investigate the effects of iron (III) ion

input variations, the amount of 0.05 M iron (III) ions placed in 0.3% HA solution was adjusted to 400–520 µL. Upon the addition of ≤ 410 µL, or ≥ 480 µL 0.05 M iron (III) ions to the HA solution, it was found that bead and thread-like precipitates were formed. In terms of efficiency, it was found that the most appropriate amount of 0.05 M iron (III) ions was between 420 µL and 470 µL without any bead- and thread-like precipitates, and more than 0.05 M iron (III) ions tended to result in a slightly smaller particle size and a slightly lower polydispersity index (PDI) in aqueous systems.

As shown in Table 3 (bottom), when 160–280 µL of 0.05 M iron (III) ions were added to the 0.1% HA solution, no significant variations in particle size were observed, but the addition of 200–300 µL of 0.05 M iron (III) ions resulted in a relatively low PDI, indicating that nanoparticles of uniform size were synthesized. In contrast, the addition of 300 µL or more of 0.05 M iron (III) ions resulted in a drastic increase in particle size and PDI, whereas the addition of 0.05 M iron (III) ions (150 µL or less) resulted in a slightly larger particle size, but a drastic increase in PDI, which indicated that irregularly sized nanoparticles were formed.

As shown in Fig. 1C, this study aimed to determine the possible influence of variation in HA % (w/v) concentration and HA concentrations of 0.3%, 0.2%, and 0.1% were tested.

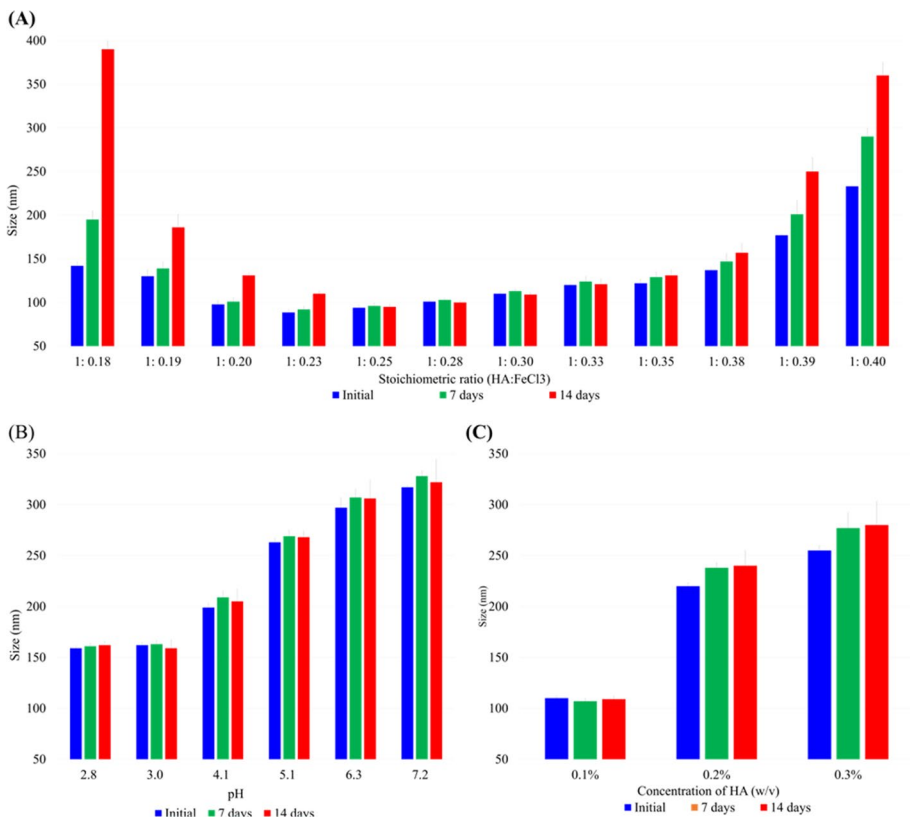

Fig. 1 Stability studies. Stability dependency on the ratio of metal ion (**A**), stability dependency on pH (**B**), and stability dependency on HA concentration (**C**). Abbreviations: HA, hyaluronan; ISHNs, irinotecan-loaded self-agglomerating hyaluronan nanoparticles

To ensure a constant *stoichiometric ratio* (HA disaccharide: iron (III) ion = 1:0.19), the volume of added iron (III) ions was adjusted to 146.7, 293.3, and 440 μL, respectively.

The lowest HA concentrations led to significantly smaller particle sizes, as shown in Fig. 1C, and we assumed that potentially, the lower HA solution concentration led to relatively lower opportunities for the combined interactions between the HA molecules directly engaged in the generation and growth of particles.

Additionally, to ascertain the physicochemical stability dependency on ionic strength, SAHNs were prepared using the methods described below. The methods changed only the ionic strength by the addition of KOH, NaOH, Na_2CO_3, and K_2CO_3 at a constant pH < 4.0. Through these preliminary studies, it was found that in general, the binding ability was reduced at high ionic strength, mainly owing to the electrostatic binding between the functional group and metal ion, as well as the higher counter ion condensation. This study also showed that a higher ionic strength typically yielded smaller particle sizes.

To determine the dependency of physicochemical stability on temperature, SAHNs were prepared using the methods described below. The methods changed the manufacturing temperature from 25 to 45 °C.

Through these preliminary studies, the reference for comparative observation of nanoparticle behavior was also measured without any temperature variation at a certain time, with regard to the instability of nanoparticles with time. Higher temperatures led to larger particle sizes, and when the temperature was returned to 25 °C, the size of nanoparticles at the exact time of temperature return was to the same as that of nanoparticles kept at the same temperature. This indicated that the size of the formed HA–iron complex nanoparticles with temperature variation was reversible.

Characterization of optimal values of SAHNs and ISHNs

The structure and morphology of the ISHNs visualized using NTA are shown in Fig. 2. The ISHNs were spherical with a relatively angular surface and displayed a less smooth spherical shape. The particle size was approximately 80–180 nm, with a maximum of 183 nm.

It was assumed that the self-agglomerating nanoparticles formed by covalent bonding were the μ-oxo form (Mercê et al. 2002) between the $FeCl_3$ and COOH groups of hyaluronan and irinotecan hydrochloride.

As shown in Table 4, the mean diameter and PDI of the SAHNs, which were determined by using DLS, were 89.8 ± 3.31 nm and 0.17 ± 0.03, respectively. In both cases, a narrow size distribution was observed. The zeta potential reflects the surface charge used to confirm the nanoparticle stability and is also important for the surface characterization of nanoparticles. The zeta potential of the SAHNs was − 31.9 ± 0.32 mV and the surface charge was negative. After lyophilization, the physicochemical characteristics (particle size, size distribution, and zeta potential) of the reconstituted SAHNs were similar to those of the SAHNs.

The reason for the assumption of μ-oxo covalent bonding in the self-agglomerating phenomenon of the nanoparticles, as shown in vials picture of Fig. 2B, it was determined by confirming the reactivity of only HA and $FeCl_3$ and aggregation by ratio in the aqueous system. In addition, as shown in Fig. 2C, the FTIR results of SAHNs, the peaks

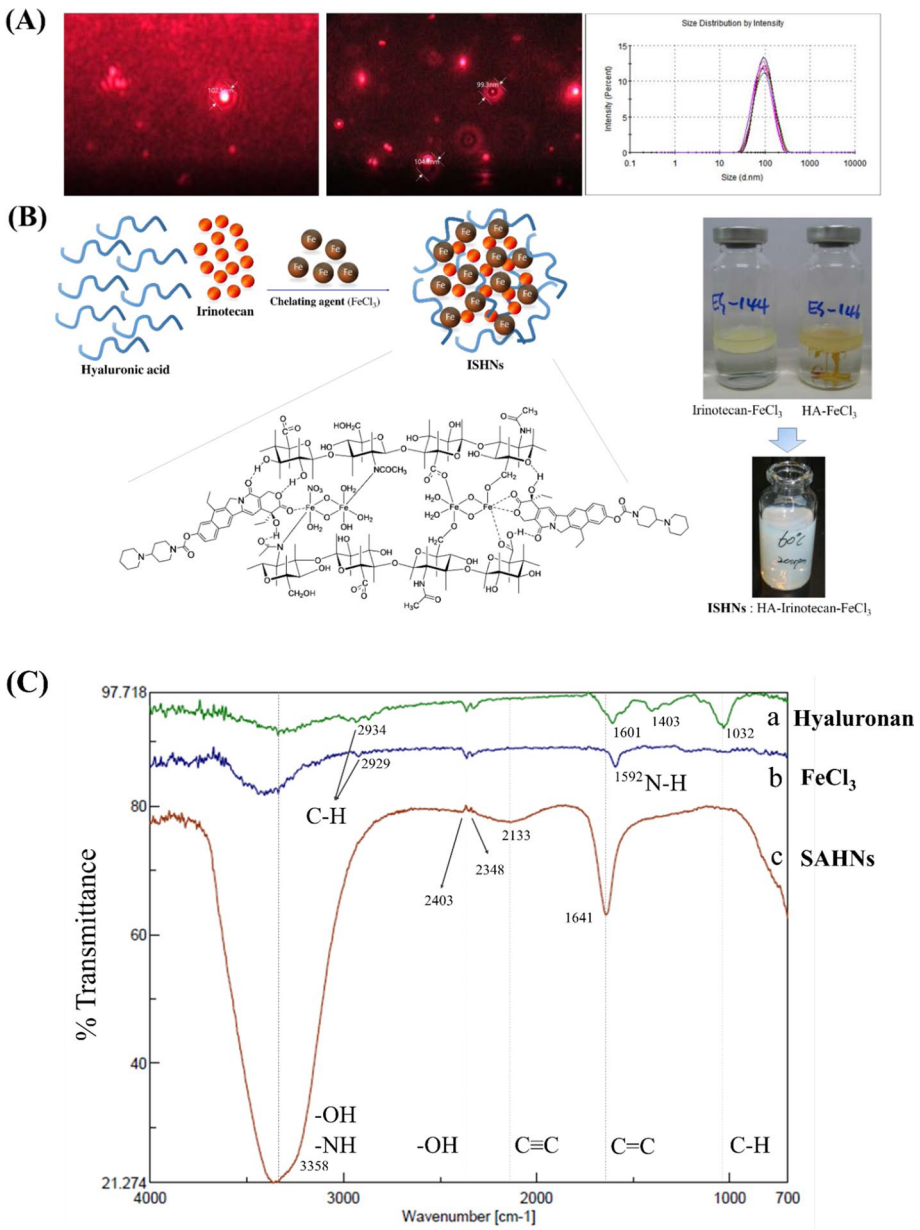

Fig. 2 **A** NTA image of the ISHNs, **B** schematic representation and illustration of the structure of ISHNs, and **C** FTIR absorption spectra of (a) hyaluronan, (b) FeCl3, and (c) SAHNs. Spectra were recorded for freshly prepared solutions without further curing treatment. NTA image scale bar = 200 nm. *HA* hyaluronin, *SAHNs* self-agglomerating hyaluronan nanoparticles, *ISHNs* irinotecan-loaded self-agglomerating hyaluronan nanoparticles, *NTA* nanoparticle tracking analysis microscope

appeared at 1641 cm^{-1} (C = C) and 2133 cm^{-1} (C≡C), and the peaks observed in a hyaluronan material disappeared at 1403 cm^{-1} and 1032 cm^{-1} (C–H). The peaks of 1641 and 2133 cm^{-1} are peaks representing double and triple covalent bonds. We confirmed that the structure of SAHNs was changed due to the change in molecular motion. Therefore, we assumed that the self-agglomerating nanoparticles were bound in the form of μ-oxo by covalent bonding.

Table 4 Physicochemical properties of optimal SAHNs and ISHNs. The data are expressed as the mean ± SD ($n = 3$)

	Formulation	Mean diameter (nm)	Polydispersity index (PDI)	Zeta potential (mV)	Encapsulation efficiency (%)[a]	Drug-loading efficiency (%)[b]	Drug content (mg/mL)[c]
Before lyophilization	SAHNs	89.3 ± 3.31	0.17 ± 0.03	− 31.9 ± 0.32	–	–	–
	ISHNs	93.8 ± 4.48	0.19 ± 0.02	− 36.3 ± 0.28	58.3 ± 0.15	25.1 ± 0.09	1.75 ± 0.11
After lyophilization	SAHNs	87.5 ± 4.09	0.20 ± 0.05	− 31.2 ± 0.25	–	–	–
	ISHNs	95.2 ± 5.56	0.21 ± 0.03	− 36.6 ± 0.41	57.3 ± 0.08	24.7 ± 0.07	1.72 ± 0.29

SAHNs self-agglomerating hyaluronan nanoparticles, *ISHN* irinotecan-loaded self-agglomerating hyaluronan nanoparticles

[a] Encapsulation efficiency (%) = (amount of irinotecan hydrochloride encapsulated in ISHNs/amount of the feed source of irinotecan hydrochloride) × 100%

[b] Drug-loading efficiency (%) = (amount of irinotecan hydrochloride in ISHNs/amount of the feed source and irinotecan hydrochloride) × 100

[c] Drug content (mg/mL) = (amount of irinotecan hydrochloride in ISHNs/amount of the feeding material and irinotecan hydrochloride in a 15-mL vial)

The mean diameter and the PDI of the ISHNs were determined by using DLS and were 93.8 ± 4.48 nm and 0.19 ± 0.02, respectively. In both cases, a narrow size distribution was observed. The zeta potential of the ISHNs was − 36.8 ± 0.28 mV and had a negative surface charge; that is, there was a negative mean charge on the hyaluronan present on the outer surface of the SAHNs and ISHNs. The mean particle size of the ISHNs was much larger than that of the SAHNs ($P < 0.05$) owing to the presence of irinotecan. The ISHNs were 5–7 nm larger than the SAHNs.

After lyophilization, the physicochemical characteristics (particle size, size distribution, and zeta potential) of the reconstituted ISHNs were similar to those of the ISHNs before lyophilization, as shown in Table 4.

It is known that particle size alters pharmacokinetics by altering tissue distribution and excretion (Maeda et al. 2013). Nanoparticles below 200 nm show increased drug accumulation in tumor cells because of the EPR effect (Fang et al. 2011). In our study, given that the size of the SAHNs and ISHNs was maintained at less than 110 nm, irinotecan accumulation of tumor cells was anticipated to be relatively high. Both the SAHNs and ISHNs had a rigid angular spherical shape, and as they are nanoparticles of HA, they had a negative charge (Table 1). These data suggest that the core of the ISHNs contained an irinotecan with a hydroxyl group and that the outside was made with HA in the μ-oxo form covalently bound to $FeCl_3$ (ferric chloride) in the aqueous phase. These nanoparticles, such as ISHNs, play an important role in the targeting of NSCLC cells. Overall, the zeta potential, particle characteristics, and morphology of the SAHNs and ISHNs were very similar, but the slight difference in particle size was presumably due to the inclusion of irinotecan HCl.

As shown in Table 2, the drug-loading efficiency (LE) and encapsulation efficiency (EE) of the ISHNs ($n = 3$) were 25.1% ± 0.09% and 58.3% ± 0.15%, respectively. After reconstitution, the EE and LE of the ISHNs (n = 3) were 57.3% ± 0.08% and 24.7% ± 0.07%, respectively. These results were satisfactory and reproducible. The yield of drug fixation reached 50–60% in the ISHNs. The EE was > 58.3% and was independent of the irinotecan content (1.75 mg/mL) for all batches of the ISHNs tested. These data suggested that

irinotecan was most conjugated in the HA-agglomerated mixture of SAHNs. During preliminary studies, we determined that the drug content in the ISHNs was > 2 mg/mL; however, to maintain stability over time, we used < 1.7 mg/mL of irinotecan for these studies.

Stability studies

To investigate the effects of the variation in proportions on the preparation of the HA–iron complex nanoparticles, iron (III) ions were added to 15 mL HA solution, and the experiments were conducted with constant stirring rate at ambient temperature and 250 rpm for 5 min. The methods changed only the stoichiometric ratio (HA disaccharide: iron (III) ion [ferric chloride]); the amount of added iron (III) ion to hyaluronan was adjusted from 1:0.18 to 1:0.40.

The SAHNs and ISHNs were reconstituted using water for injection, to obtain solutions at a concentration of 1.7 mg/mL irinotecan hydrochloride.

The results of the stability dependency of ISHNs on the ratio of metal ions were evaluated by their change in size, as shown in Fig. 2A. The reconstituted ISHNs without stabilizers were physically unstable when stored at 25 °C for 14 days. The size of the tested parameters of the nanoparticles (appearance, particle size, and SD) increased when stored at 25 °C for 14 days. Overall, they tended to increase in size. However, when between 1:0.25 and 0.35 of the stoichiometric ratio (HA:$FeCl_3$) were added into the 0.1% HA solution, no significant variations in particle size were observed.

The results of the stability dependency of ISHNs on pH were evaluated by their change in size over 14 days, as shown in Fig. 2B. Although the particle size was initially determined by the pH, there was no change in particle size over time. The reconstituted ISHNs were physically stable in solutions of various pH values stored at 25 °C for 14 days. As shown in Fig. 2B, the nanoparticles showed no increase in the tested parameters (pH, appearance, particle size, and SD) when stored at 25 °C for 14 days. Overall, there was no tendency for the parameters to increase.

The results of the stability dependency of ISHNs on the concentration of HA exhibited between 0.1% and 0.3% are shown in Fig. 2C and were evaluated by their change in size over 14 days. The initial particle size differed depending on the concentration of HA and was stable at 0.1% HA, but gradually increased over time at concentrations of 0.2% or more. In our previous experiments, we studied the stability dependency of the ionic strength and temperature. Although the particle size was initially determined by the ionic strength and temperature, it did not change over time. The reconstituted ISHNs were physically stable in solutions of various ionic strengths when stored at 25 °C for 14 days.

The results of the stability analysis for the total height of samples filled in a cylindrical glass cell using Turbiscan Lab® are shown in Fig. 3 and represent the solution stability. The results were measured and illustrated as transmission flux (%) because both samples were of low concentration. Accordingly, the results of the analysis are presented in the comparison of transmission flux (%) vs. sample height. As shown in Fig. 3A, the reconstituted ISHNs without stabilizer were physically unstable in the test of solution when stored at 25 °C for 24 h. However, as shown in Fig. 3B, the reconstituted ISHNs with glutamic acid as a stabilizer were physically stable in the test solution when stored at

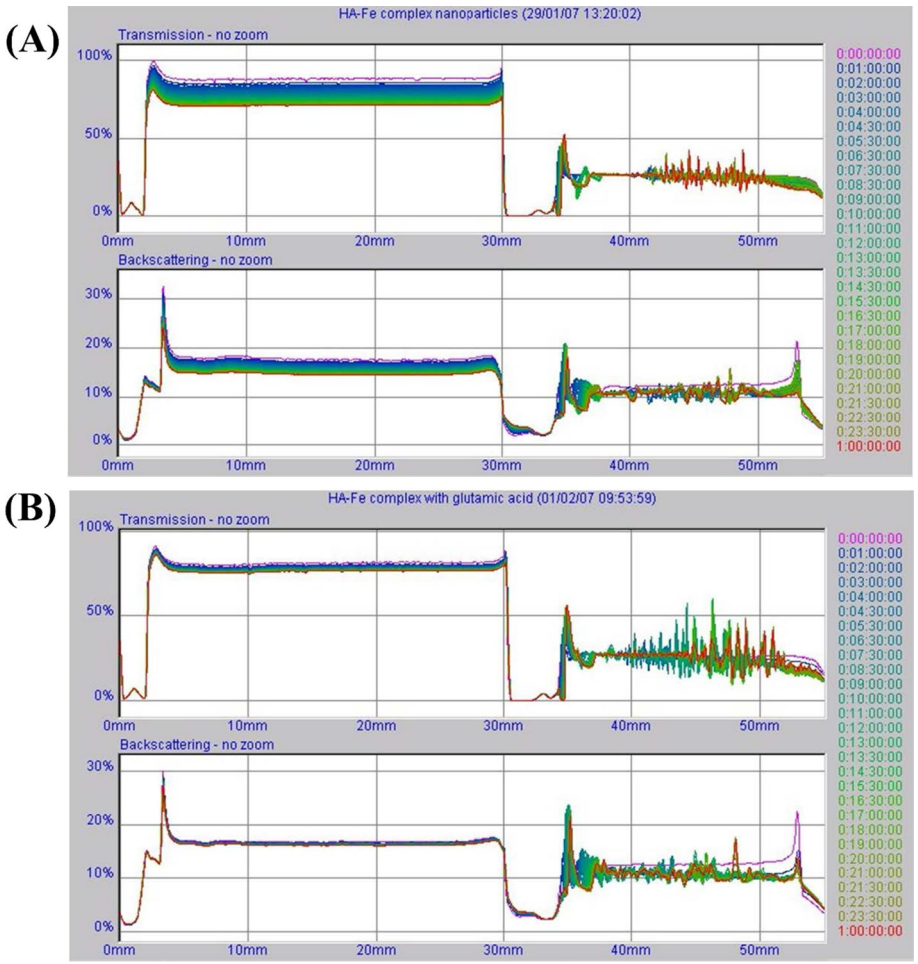

Fig. 3 Solution stability of the ISHNs. The stability analysis results for the total height of the samples filled in a cylindrical glass cell using Turbiscan Lab® for solution stability, ISHNs without L-glutamic acid as a stabilizer (**A**), and ISHNs with L-glutamic acid as a stabilizer (**B**). Abbreviations: HA, hyaluronan; ISHNs, irinotecan-loaded self-agglomerating hyaluronan nanoparticles

25 °C for 24 h. Through studies of various materials, L-glutamic acid (GA) was adopted as a stabilizer; coordination with unreacted carboxylic groups occurred in the HA chain and prevented any further growth of particles. Thus, the addition of only 0.02 M GA to the ISHNs achieved optimal results, and there was no significant variation in the size parameters at 25 °C for 7 days. That is, the adoption of glutamic acid contributed to marked stabilization, but the concentration of GA did not influence the stability, except for 0.02 M GA (Table 5). The data in the table show that higher concentrations of added GA led to a large particle size in the initial step. In particular, the application of 0.02 M GA, as shown in Fig. 3B, resulted in smaller and more stabilized uniform particle sizes.

In vitro drug release studies

The 21-h in vitro drug release patterns of ISHN 1 (manufactured with 0.02 M ferric chloride), ISHN 2 (manufactured with 0.05 M ferric chloride), and Camptosar® (irinotecan hydrochloride) in pH 7.0 PBS, as measured using the above-mentioned dialysis method,

Table 5 Characterization of SAHNs by concentration of the stabilizer L-glutamic acid

Concentration of glutamic acid (M)	Initial		1 day		2 days		4 days		7 days	
	Size*	% SD	Size	% SD	Size	% SD	Size	% SD	Size	% SD
0.00	108.5	3.45	219.8	1.08	232.0	3.13	243.8	5.47	262.3	6.56
0.01	126.3	2.74	146.0	0.84	153.5	1.64	160.8	3.09	166.8	4.89
0.02	147.7	3.28	154.0	1.15	160.0	2.22	161.3	2.20	163.0	2.87
0.03	139.3	1.84	179.4	0.97	190.7	0.64	198.0	1.96	228.8	1.98
0.04	141.3	2.24	183.3	0.10	194.3	1.66	207.3	2.09	211.8	4.28
0.05	180.0	2.67	185.3	1.01	197.0	1.44	238.3	2.19	219.7	4.44

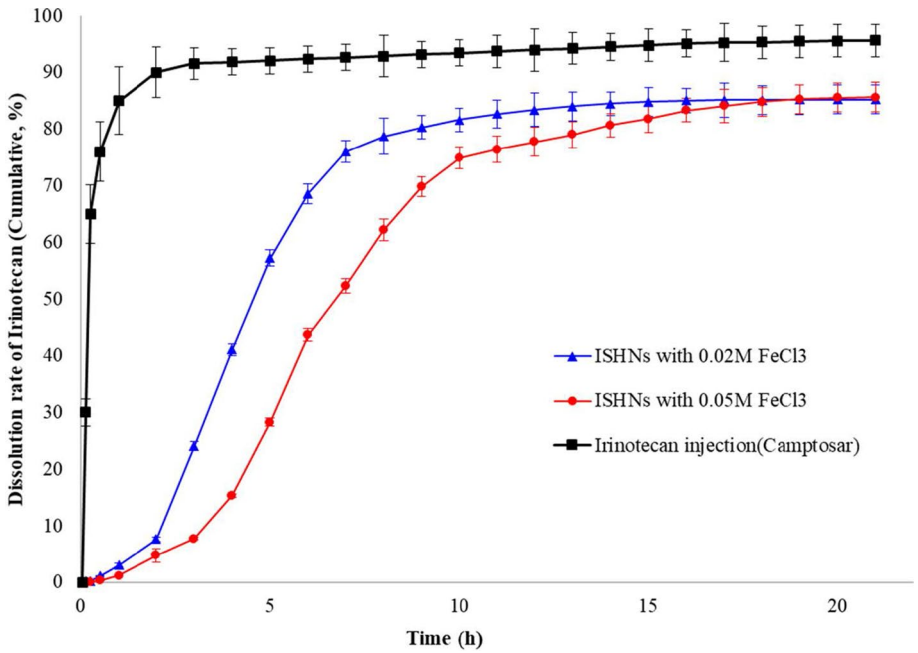

Fig. 4 In vitro drug release studies. In vitro drug release of ISHNs and irinotecan injection. The release of irinotecan hydrochloride was determined at a pH of 7.0. Data are expressed as mean ± SD ($n = 3$)

are shown in Fig. 4 (Zhao et al. 2012; Yang et al. 2013, Cho and Park 2014). The Camptosar® injection released > 90% of irinotecan within 2 h, whereas the ISHNs released < 10% after 2 h and approximately 75% after 10 h. The ISHNs made with 0.02 M and 0.05 M $FeCl_3$ resulted in a sustained release pattern in which the irinotecan hydrochloride was continuously released from the hyaluronan self-agglomerated nanocarriers and displayed significantly different release characteristics than those of the Camptosar® injection. Further, the release pattern of the ISHNs made with 0.05 M $FeCl_3$ was sustained for a longer period than that of the ISHNs made with 0.02 M $FeCl_3$. These results indicated that the in vitro release of irinotecan hydrochloride was affected by the bonding between hyaluronan, irinotecan, and ferric chloride, as determined by the concentration of ferric chloride. We assumed that the ISHNs may circulate, and that retention would be higher than that for an irinotecan injection into cancer cells for an extended period after administration. Considering the time required for the formulations to reach the

cancer cells after administration in the body, a sustained release of the drug would be more advantageous than a rapid-release formulation and offer greater therapeutic benefits (Cho and Park 2014). Therefore, ISHNs may be more efficient for the delivery of drugs via targeted release than Camptosar® injection.

In vitro NSCLC cell-targeting studies

The results of the in vitro NSCLC cell targeting CD44 exhibited by the SAHNs, which were used to evaluate their ability to target cancer cells that generally overexpress CD44 (Taurin et al. 2012) are shown in Fig. 5. We used two human NSCLC cell lines, H23 ($CD44^+$) cells, which express CD44 on their surface, and A549 ($CD44^-$) cells, which do not express CD44 (Leung et al. 2010).

The results of the in vitro NSCLC cell uptake of the SAHNs for CD44 receptor, which was performed to assess the cell-targeting capability of these nanoparticles toward human NSCLC cells that generally overexpress CD44, are shown in Fig. 5.

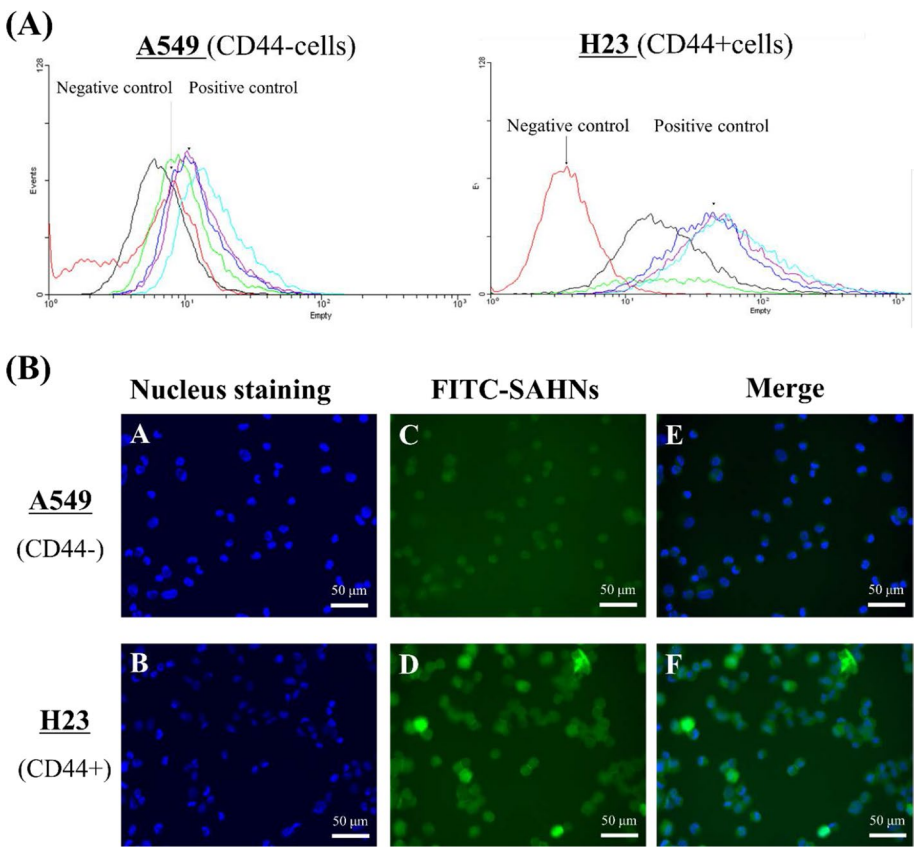

Fig. 5 In vitro cancer cell targeting studies of the SAHNs. **A** Fluorescence-activated cell sorting (FACS) was performed in A549 cells and H23 cells of the human non-small cell lung cancer cell lines. FITC-labeled SAHNs were prepared with 0.1% (w/v) HA. **B** Confocal microscopy images of A549 (CD44-negative) and H23 (CD44-positive) NSCLC cells incubated with FITC-labeled SAHNs. 20 μg/mL FITC-conjugated SAHNs were added to each H23 and A549 cells line (1×10^6 cells), which was then incubated at 37 °C for about 4 h (scale bar = 50 μm). Notes: Fluorescent images of the cell nucleus stained by Hoechst 33,342 (white A, B), fluorescent images of FITC-SAHNs with green fluorescence in cells (white **C**, **D**), and fluorescent images of the FITC-SAHNs fluorescence superimposed on the nucleus and green fluorescence in cells (white **E**, **F**). *HA* hyaluronan, *SAHNs* self-agglomerating hyaluronan nanoparticles

None of the samples used for the in vitro cell studies included ISHNs with an irinotecan, because our team could not evaluate the precise cell count as cell death was observed following the administration of ISHNs containing anticancer agents such as irinotecan hydrochloride in cell-targeting studies.

As shown in Fig. 5A, the results of the in vitro NSCLC cell affinity studies of the SAHNs for CD44 using A549 ($CD44^-$) cells revealed that specific affinity binding was not observed in all the specimens tested. The in vitro NSCLC cell affinity test of the SAHNs in A549 ($CD44^-$) cells showed that the SAHNs had no specific binding to CD44 present on the NSCLC cells. In contrast, SAHNs showed substantial specific uptake binding to H23 ($CD44^+$) cells (Fig. 5A, bottom). SAHNs had a targeting capability to H23 cells fivefold higher than that of A549 cells that do not have CD44. Therefore, SAHNs containing HA on the outer surface of the nanoparticles might offer an outstanding drug delivery system for passive and active tumor targeting.

As shown in Fig. 5B, the images of the in vitro cellular uptake and specific affinity of the SAHNs in the H23 and A549 cells were captured using confocal microscopy. The pictures were of single sections through A549 and H23 cells. The left picture panels, which show nuclear cell staining, were obtained from the blue cell channel. The center picture panels, which show the fluorescence of encapsulated FITC, were obtained from the green channel; and the right picture panels are merged pictures from the previous two images. Although SAHN-treated A549 cells did not show any specific binding and cellular uptake, the SAHN-treated H23 cells displayed outstanding cellular uptake and specific affinity binding. The results demonstrate the theory behind the ligand–receptor reaction between HA and CD44. As shown in Fig. 5, the results from SAHNs were consistent with confocal microscopy and fluorescence-activated cell sorting (FACS) data, which suggested that SAHNs with HA facilitate attachment to CD44-overexpressing cells in human NSCLC cells. The results of FACS and confocal microscopy indicate that the cell affinity of SAHNs should be sufficient to result in efficient cell binding and uptake via CD44 in NSCLC cells. Therefore, it was shown that the SAHNs with HA are a remarkable drug delivery system for passive and active tumor targeting.

Cell viability studies

The A549 and H23 cells were cultured with: (1) HA solution, (2) SAHNs, (3) ISHNs, and (4) irinotecan at 0.3 to 30 μM concentration for 48 h to examine the cell viability by WST-1 assay. As shown in Fig. 6A, it can be seen that the A549 cell viability of the groups treated with SAHNs and ISHNs were 60.9 ± 0.38 and $52.5 \pm 2.31\%$ at the concentration of 30 μM, respectively. However, it can be seen that the cell viability of the groups treated with irinotecan was $20.6 \pm 0.14\%$ at a concentration of 30 μM.

As shown in Fig. 6B, it can be seen that the H23 cell viability of the groups treated with SAHNs and ISHNs were 88.9 ± 3.17 and $78.5 \pm 1.73\%$ at a concentration of 30 μM, respectively. However, it can be seen that the cell viability of the groups treated with irinotecan solution was $23.8 \pm 0.17\%$ at a concentration of 30 μM.

Overall, SAHNs and ISHNs treated with 30 μM in A549 cells showed a 50% survival rate. However, in H23 cells, SAHNs and ISHNs treated with 30 μM showed a survival rate of approximately 80%. When compared with nanoparticles and irinotecan, A549 cells showed more than two times higher cell viability, and H23 cells showed

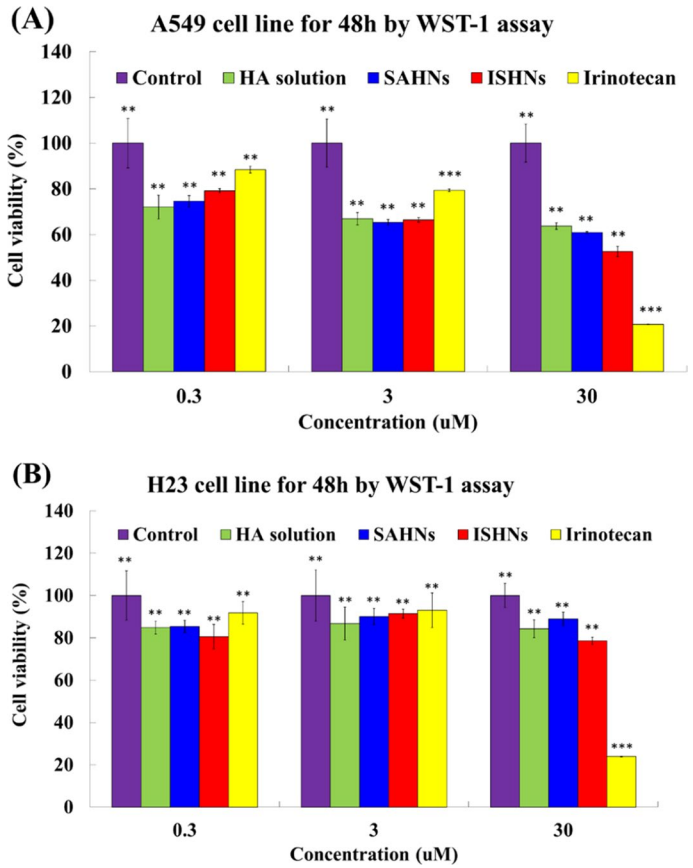

Fig. 6 Cell viability studies. Cytotoxicity of self-agglomerating nanoparticles on A549 and H23 cells analyzed by WST-1 assay. Results indicate the cell viability (%) level (an average of three separate samples on the plate), which relates to the amount of live or viable cells for each treated sample at various concentrations (0.3, 3, and 30 μM) for 48 h. The results are mean ± SD, representative of three independent experiments ($n = 3$). $^{**}p < 0.01$, $^{***}p < 0.001$, compared with control. **A** The A549 cells were cultured with (1) HA solution, (2) SAHNs, (3) ISHNs, and (4) irinotecan at 0.3 to 30 μM concentration for 48 h to examine the cell viability by WST-1 assay. **B** The H23 cells were cultured with (1) HA solution, (2) SAHNs, (3) ISHNs, and (4) irinotecan at 0.3 to 30 μM concentration for 48 h to examine the cell viability by WST-1 assay. Abbreviation: HA, hyaluronic acid; SAHNs, self-agglomerating hyaluronan nanoparticles; ISHNs, irinotecan-loaded self-agglomerating hyaluronan

approximately four times more cell viability. As expected, there was no significant difference in the cell viability of ISHN and irinotecan at low concentrations of 3 μM or less, but a significant cell viability (%) was seen at a concentration of 30 μM. These cell viability tests showed a high cell apoptosis of about 80% in the free irinotecan group, whereas the irinotecan-loading nanoparticle ISHN showed a lower cell apoptosis rate of about 48%.

Even when the same concentration of anticancer drug was administered, irinotecan in nanoparticles form showed lower cytotoxicity than free irinotecan solution. Overall, the cell viability studies with ISHN showed a very modest targeting effect on the lung cancer cells (A549 and H23). These results show that our nanoparticles are safer than free irinotecan.

However, as shown in Fig. 6a, it was confirmed that the HA solution and SAHNs had their own cytotoxic effect even in the absence of irinotecan as an anticancer drug, especially in the A549 cell line.

In addition, contrary to our expectations, HA and HA-nanoparticles were more adsorbed in H23 cells in which CD44 was overexpressed outside the cells than in A549 in which CD44 was not overexpressed outside the cell, making us assume that the cytotoxicity would be stronger (Fig. 6). However, the actual result was opposite. It is presumed that the apoptosis rate was lower because HA was attached to CD44 on the cell surface of H23, which is a CD44-positive cell, and acted outside the cell. In contrast, in the A549 cell line, it is presumed that substances such as HA or ferric chloride directly affect the cell surface.

Only the excipients constituting the HA nanoparticles showed a modest cytotoxic effect in non-small cell lung cancer cell lines. In the future, it is necessary to shift to an excipient with significantly less toxicity.

Conclusion

In this study, self-agglomerating water-soluble anticancer drug nanoparticles were successfully developed. Irinotecan hydrochloride was synthesized in HA nanoparticles using the ion binding abilities of ferric chloride was. To prepare a drug delivery system that simultaneously satisfies both passive targeting and active targeting that is highly specific and selective to cancer cells, irinotecan–hyaluronan self-agglomerating nanoparticles were selected. As the structure of HA has a carboxyl group and irinotecan has a hydroxyl group, we applied ferric chloride as the chelating technique of the μ-oxo form. Investigation of the stoichiometric ratio of HA, irinotecan HCl, and iron (III) ions revealed the production of ISHNs with excellent stability at specific stoichiometric ratios. Through characterization studies of ISHNs, we identified their physicochemical properties and optimized the self-agglomeration to yield hyaluronan nanoparticles with excellent stability.

Thus, we developed irinotecan-loaded ISHNs, which comprised irinotecan HCl as a water-soluble anticancer agent, HA as a targeting moiety, $FeCl_3$ as a binder for self-agglomeration, and GA as a stabilizer; HA is a binding material for CD44 in NSCLC cells. The ISHNs had a negatively charged surface that was fabricated with hyaluronan itself by a covalent bond using the μ-oxo form of hyaluronan, irinotecan, and ferric chloride in the aqueous solution to actively target cancer cells. In the results of in vitro drug release studies, we proposed that the ISHNs may circulate and be retained for longer than irinotecan injection in cancer cells for an extended period after administration. The water-soluble anticancer drug-loaded nanoparticles did not dissociate immediately upon administration in aqueous solution and also improved the stability of the formulation. The in vitro cancer cell targeting study of self-agglomerating nanoparticles to CD44 overexpressed human cancer cells was relatively higher than that to CD44-negative cells. The HA-agglomerated nanoparticles provided remarkable targeting capability for NSCLC cells based on an in vitro NSCLC cell targeting study. Furthermore, the ISHNs had a stable particle size of approximately 90 nm, with a narrow size distribution, and were loaded with 1.75 mg/mL of irinotecan HCl inside the hyaluronan-agglomerated complex. In conclusion, these ISHNs were easily manufactured, contained a high

payload of water-soluble anticancer agents, and displayed excellent stability and the capability to deliver a water-soluble anticancer agent to tumor cells.

Materials and methods

Materials

Injectable grade sodium hyaluronate (Na-HA) was provided by Bioiberica Co., Ltd. (Barcelona, Spain) and Kibun Food Chemifa Co., Ltd. (Kamogawa, Japan), with molecular weights of approximately 0.5, 0.8, 0.95, 1.5, and 3.6 MDa. Irinotecan hydrochloride of sterilized injectable grade was purchased from Liangyugang Jari Pharmaceutical Co., Ltd. (Shanghai, China). Unites States Pharmacopeia (USP) irinotecan hydrochloride RS was purchased from the United States Pharmacopeial Convention Inc. (Rockville, MD, USA). Ferric chloride ($FeCl_3$) anhydrous, D-glutamic acid, and phosphate buffer were purchased from Sigma-Aldrich Chemical Co., Ltd. (St. Louis, MO, USA). Ethanol (99.9%), phosphoric acid, and hydrochloric acid were purchased from Duksan Chemical Co., Ltd. (Gyeonggi, Korea). Methanol (99.9%), HPLC-grade acetonitrile, and 0.22 μm membrane filters were purchased from Merck Millipore (Billerica, MA, USA). Camptosar® (irinotecan hydrochloride injection) was purchased from Pfizer Inc. (New York, NY, USA). H23 ($CD44^+$)-expressing human NSCLC cell lines and A549 ($CD44^-$) human NSCLC cell lines were acquired from the Korean Cell Library Bank (KCBL) and the American Type Culture Collection (ATCC; Manassas, VA, USA).

Heat-inactivated fetal bovine serum (FBS), N-2-hydroxyethylpiperazine-N-2-ethanesulfonic acid (HEPES), RPMI 1640 cell culture medium (Waymouth), streptomycin, and penicillin were purchased from Gibco Technologies, Inc. (Big Cabin, OK, USA). All chemicals were of reagent grade and used without further purification.

Preparation of SAHNs

The SAHNs comprised ferric chloride, HA, D-glutamic acid, and water for injection. First, the nanoparticles, which were composed of HA and ferric chloride, were selected based on their compatibility and solubilizing capability. Irinotecan hydrochloride was used as the model hydrophilic anticancer drug. d-Glutamic acid was chosen as the stabilizer, owing to its reconstituted stability and stability in aqueous solution. Moreover, these materials are known to have low toxicity, excellent biodegradability, and biocompatibility in other research studies (Liang et al. 2016; Kim et al. 2017; Kim et al. 2017). The quantities of HA, ferric chloride, and glutamic acid in the SAHN formulation were 0.1%, 260 μL, and 800 mg, respectively. SAHNs were prepared by chelating the μ-oxo form via ionic bonding (Mercê et al. 2002). Briefly, for the extraction of only hyaluronan, 12 g sodium HA (molecular weight: 950,000) was dispersed in 3.0 L of a 7:3 mixture of 99.9% ethanol and 0.1 M HCl solution. The resulting dispersion was kept at 25 °C in a 3.0 L beaker and mechanically stirred at 400 rpm for 24 h to reach an equilibrium state and filtered through a 0.45 μm RC membrane filter. The sodium HA remaining on the filter was washed three times with 99.9% ethanol and dried in a vacuum desiccator to extract only HA. The obtained HA was confirmed by pH measurement from pH 2.6 to 2.8, and analysis using an FT-IR instrument (Brookfield, NJ, USA) to confirm the presence of a salt peak.

To prepare a stabilized solution of 0.1% HA, 15 mg of HA was added to 15 mL of 0.02 M D-glutamic acid solution made with water for injection. Thereafter, while stirring the stabilized 0.1% HA solution at 250 rpm with a mechanical stirrer, between 140 and 320 μL of 0.05 M ferric chloride solution was added (stirring was continued for 30 min), and the solution was cooled to 20 °C.

To prepare a stabilized 0.3% HA solution, 45 mg of the obtained HA was added to 15 mL of 0.02 M D-glutamic acid solution made with water for injection. Thereafter, while stirring the stabilized 0.3% HA solution at 250 rpm with a mechanical stirrer, 400–520 μL of 0.05 M ferric chloride solution was added (stirring was continued for 30 min), and then the solution was cooled to 20 °C. Finally, the two types of prepared SAHN solutions were lyophilized using a freeze dryer (Virtis lyophilized dryer™, Warminster, PA, USA).

Preparation of irinotecan-loaded self-agglomerating hyaluronan nanoparticles (ISHNs)

The ISHNs comprised ferric chloride, HA, glutamic acid, irinotecan hydrochloride, and water for injection. For the extraction of only hyaluronan, 12 g sodium HA (molecular weight: 950,000) was dispersed in 3.0 L of a 7:3 mixture of 99.9% ethanol and 0.1 M hydrochloride solution. The resulting dispersion was kept at 25 °C in a 3.0 L beaker and mechanically stirred at 400 rpm for 24 h to reach an equilibrium state and filtered through a 0.45 μm RC membrane filter. The sodium HA remaining on the filter was washed three times with 99.9% ethanol and dried in a vacuum desiccator to extract only HA. The obtained HA was confirmed by pH measurement from pH 2.6 to 2.8, and analysis using an FT-IR instrument (Brookfield, NJ, USA) to confirm the presence of a salt peak.

To prepare a stabilized mixed solution with irinotecan and HA, 15 mg of HA and 45 mg irinotecan hydrochloride were added to 15 mL of 0.02 M glutamic acid solution made with water for injection. Thereafter, the mixture was heated to approximately 60 °C and stirred until an aqueous solution was obtained and then cooled to 25 °C. The pH was adjusted to approximately 5.0, using 2 N sodium hydroxide. Thereafter, while stirring the stabilized 0.1% HA solution at 200 to 400 rpm with a mechanical stirrer, 200 μL of 0.05 M ferric chloride aqueous solution was added (stirring was continued for approximately 1 h), and then the solution was cooled to 20 °C. Finally, the prepared ISHNs were lyophilized using a freeze dryer (Virtis lyophilized dryer™, Warminster, PA, USA).

Characterization of SAHNs and ISHNs

Zeta potential, particle size, and polydispersity

The physical properties of the particles (zeta potential, size, and polydispersity) of the SAHNs and ISHNs were measured at 25 °C using a laser scattering particle analyzer using dynamic light scattering (DLS) methods (Model: Zetasizer NanoZS™, Malvern, UK). The reconstituted solutions of SAHNs and ISHNs were diluted 10 times with distilled deionized water and sample measurements were performed at 25 °C, with a minimum of three replicates(Kim and Park 2017a, b).

Morphology

The morphology of the ISHNs was monitored using a nanoparticle tracking analysis (NTA) microscope (NanoSight LM10, Malvern panalytical, Amesbury, UK), equipped with a sample chamber with a 640-nm laser and a Viton fluoroelastomer O-ring. The NTA was operated in the solution state to analyze the samples. The samples were injected into the sample chamber with sterile syringes (BD Discardit II, New Jersey, USA) until the liquid reached the tip of the nozzle. All measurements were performed at room temperature using live monitoring heat stress measurements.

FTIR

Fourier transform infrared (FTIR) spectra of the self-agglomerating nanoparticles formed by the μ-oxo covalent bond were recorded using a PerkinElmer Spectrum 100 instrument with an attenuated total reflection (ATR) sampling accessory, where the drops were applied to the sensor top plate of the instrument. The spectra were recorded from 4000 to 600/cm with a resolution of 4/cm, averaging four scans. The spectra were normalized and are presented as the transmittance (%) units. The results are presented in the range of 3000–1000/cm, within which the bands of most interest appear (Kim and Lee 2017).

Stability studies

Solution stability

Turbiscan Lab® (Formulaction, France) was used to determine the physical solution stability of SAHNs and ISHNs in an aqueous solution. Transmission light was used as a clear liquid. These solution samples were prepared in a 20 mL glass vial (height: 30 mm) for Turbiscan Lab® equipment. The signal value was obtained at every 40 μm throughout the sample. The characteristic analysis of the aggregation behavior was monitored by the measurement of backscattered monochromatic light ($\lambda = 880$ nm) using a Turbiscan Lab® (Formulaction, Toulouse, France) in an aqueous system. The samples were placed in flat-bottomed cylindrical glass tubes (27.5 mm external diameter, 70 mm height) placed in the instrument, and the backscattered light from the solutions, including SAHNs and ISHNs, was measured at 25 °C periodically along the length of the tube(Kim and Park. 2017a, b).

Physicochemical stability

To ascertain the physicochemical stability, the SAHNs and ISHNs were reconstituted with water for injection. The change in particle size and zeta potential was evaluated on the first day of storage, and after 7 and 14 days of storage at 25 °C.

Stability dependency on the ratio of metal ions

To ascertain the physicochemical stability dependency on the ratio of the metal ion to HA, SAHNs and ISHNs were prepared using the methods described below. However, the methods changed only the stoichiometric ratio (HA disaccharide: iron (III) ion

[ferric chloride]), and the amount of added iron (III) ion to hyaluronan was adjusted from 1:0.18 to 1:0.40.

The SAHNs and ISHNs were reconstituted with water for injection to obtain solutions at a concentration of 1.7 mg/mL irinotecan HCl.

Stability dependency on pH

To ascertain the physicochemical stability dependency on the pH value, SAHNs and ISHNs were prepared using the methods described below. The methods changed only the manufacturing pH between 2.8 and 8.0, by the addition of K_2CO_3.

Stability dependency on HA concentration

To ascertain the physicochemical stability dependency of the concentration of HA, SAHNs and ISHNs were prepared using the methods described below. The methods changed only the HA concentration between 0.1% and 0.3%. The SAHNs and ISHNs were reconstituted with water for injection. The change in particle size and zeta potential was evaluated on the first day of storage, and after 7 and 14 days of storage at 25 °C.

Effect of stabilizer

SAHNs and ISHNs were prepared using the methods described below to ascertain the effect of stabilizers on the nanoparticles. The methods changed only the concentration of L-glutamic acid from 0.01 to 0.05 M. Thereafter, the SAHNs and ISHNs were reconstituted with water for injection. The change in particle size and polydispersity index was evaluated on the first day of storage, and after 1, 2, 4, and 7 d of storage at 25 °C.

HPLC analysis

The content of irinotecan hydrochloride was assayed using a HPLC system, which was equipped with a 255 nm detector and a separation module (Waters 1525/5950 series, CA, Singapore, and USA). A C_{18} silica column (Waters, 4.6 mm × 250 mm, 5 μm) was used for the analysis, and the temperature was maintained at 40 °C. The mobile phase, which consisted of phosphate buffer, methanol, and acetonitrile (59:24:17, v/v), was filtered through a 0.22 μm membrane and degassed using an online N_2 degasser. The diluent solution was prepared using a mobile phase adjusted with diluted hydrochloric acid to achieve a pH of 3.65 ± 0.15. The flow rate was 1.5 mL/min, and the injection volume was 15 μL. The tailing factor was not more than 1.5, and the relative standard deviation (RSD) for replicate injections was not more than 2.0%. After accurately weighing 10 mg irinotecan hydrochloride, the assay samples were prepared by dissolution of the sample and then by dilution of the stock with the diluent to obtain concentrations between 0.05 and 1 mg/mL. The standard deviation (SD) of precision and accuracy was < 2%. The calibration curve was rectilinear, with a correlation coefficient of 0.999. Thereafter, the standard solution was dissolved in an accurately weighed quantity of USP irinotecan HCl RS in *Diluent* to obtain a solution with an approximate concentration of 1 mg/mL. The assay solution was dissolved in an accurately weighed quantity of irinotecan HCl in *Diluent* to obtain a solution with a concentration of approximately 1 mg/mL.

LE and EE in ISHNs

To evaluate the EE and LE, 2 mL each of the ISHNs was filtered through a 0.22 μm Acro Disk membrane filter (Emflon Membrane® II of Acro Disk 50 Devices, Pall Corp., NY, USA) to remove any unencapsulated irinotecan hydrochloride, which was soluble in the water phase. Subsequently, 1 mL of the filtrate (indirect sample) was measured using the HPLC method described below. Then, 0.05 g of the non-filtrate (ISHNs) was centrifuged at 65,000 *g* for about 1 h using a Beckman TL 100 Ultracentrifuge (Beckman Coulter, CA, USA) to obtain the entrapped irinotecan hydrochloride in the ISHNs. The centrifuged precipitant was dissolved in 0.05 mL acetonitrile and the drug content encapsulated in the ISHNs was subsequently measured using the HPLC assay method described below (Kim and Park 2017b, c).

The amount of irinotecan hydrochloride entrapped in the ISHNs was calculated using the following equations:

EE (%) = (amount of irinotecan hydrochloride encapsulated in ISHNs/amount of feeding irinotecan hydrochloride) × 100.

LE (%) = (amount of irinotecan hydrochloride in ISHNs/amount of feeding material and irinotecan hydrochloride) × 100.

In vitro release studies

The 21 h in vitro release studies of ISHN 1 (manufactured with 0.02 M ferric chloride), ISHN 2 (manufactured with 0.05 M ferric chloride), and Camptosar® (irinotecan hydrochloride injection) were evaluated by using a previously described dialysis method (Cho and Park. 2010). Dialysis membranes (Spectra/Por MW 10,000–12,000, CA, USA) were stabilized by immersion in the releasing medium (2% sodium bicarbonate and 1 mM EDTA in 1 L of ddH_2O) for approximately 40 min before use. Subsequently, 2 mL of the reconstituted ISHNs (ISHN 1, 1.72 mg/mL; and ISHN 2, 1.74 mg/mL) was added to the dialysis tubing attached to a paddle of dissolution tester, and the release of irinotecan was determined according to apparatus 2 of the USP dissolution method (paddle method). The release test was performed with 350 mL of the release medium at 50 rpm and 37 °C; 1 mL of the released sample was collected at each time point (0.0416, 0.125, 0.25, 0.5, 1, 2, 3, 4, 5, 6, 7, 8, 9, 10, and every hour for up to 21 h). The content of irinotecan in each sample was measured using the HPLC method described below. The release medium was continuously replenished to maintain a volume of 350 mL. To compare the release patterns, the diluted 3.5 mg/mL Camptosar® (100 mg/5 mL) was placed into the dialysis tubing attached a paddle of dissolution tester and the release of irinotecan hydrochloride was measured by using the same method as described for the irinotecan release measurements.

In vitro cancer cell-targeting studies

To determine the specific cancer cell affinity of SAHNs for CD44, H23 and A549 cells were used as model NSCLC cells. CD44 is highly expressed on the surface of H23 cells, but not in A549 cells (Leung et al. 2010). The cells were cultured in RPMI 1640 medium supplemented with 10% (v/v) FBS, 100 U/mL penicillin, and 0.1 mg/mL streptomycin and exposed to a humidified atmosphere of 5% CO_2 at 37 °C. To detect the binding affinity using a fluorescence method, FITC was conjugated to the SAHNs using the following

method. FITC-labeled SAHNs were obtained by conjugation to 0.2 mg FITC instead of irinotecan hydrochloride using the preparation method for the SAHNs. The unlabeled fluorescent material was removed using a cassette-type dialysis membrane (Pierce, MW cutoff: 2000). Subsequently, 20 μg/mL FITC-conjugated SAHNs were added to each H23 and A549 cell line (1×10^6 cells), which were then incubated at 37 °C for approximately 4 h. After incubation, each H23 and A549 cell line was washed 2 times with PBS (pH 7.4) and treated with 0.1% trypsin for approximately 2 min. H23 and A549 cells were washed thrice with PBS (pH 7.4) supplemented with preservatives (0.2% FBS and 0.02% sodium azide), and then fixed with 400 μL 4% paraformaldehyde for 10 min. To determine the affinity to CD44, the NSCLC cells were treated with FITC-conjugated SAHNs and then analyzed using cell-related fluorescence at emission and excitation wavelengths (λ) of 520 and 488 nm, respectively, by FACS (Becton-Dickinson FACScalibur, NJ, USA). The cellular uptake and specific binding of SAHNs were visualized using a confocal microscope (Olympus LSM 510, Tokyo, Japan).

Cell viability studies

A549 and H23 cells (5×10^3) were seeded in each well of a 96-well culture plate and incubated for 24 h. Each of the SAHNs (0.3 to 30 uM) and inactive ingredients which were added into each well was removed, and the plate was washed with PBS. WST-1 (100 uL) was added to each well and incubated at 37 °C for 2 h. The 96-well culture plate was mounted on an ELISA reader (BioTek, Epoch microplate spectrophotometer, VT, USA) and optical density (OD) was measured at 450 nm. The analysis was performed using Gen5™.

Statistical analysis

Data are expressed as mean (x) ± SD. The comparison of the mean between groups was conducted using single factor variance analysis, and the LSD test was used for pairwise comparison. Differences were considered statistically significant at P values of ≤ 0.05. The Minitab® (Version 18, Minitab Inc., PA, USA) software was used for all statistical analyses.

Abbreviations

HA: Hyaluronan; SAHNs: Self-agglomerating hyaluronan nanoparticles; ISHNs: Irinotecan-loaded self-agglomerating hyaluronan nanoparticles; NSCLC: Non-small-cell lung cancer.

Acknowledgements

Not applicable

Authors' contributions

JE designed the experimental protocols, performed the experiments, and analyzed the results. JE and YJ wrote the manuscript. JE and YJ revised the manuscript. All authors reviewed the final draft of the manuscript. All authors read and approved the final manuscript.

Funding

This study was supported by a National Research Foundation of Korea (NRF) grant funded by the Korean government (NRF-2018R1C1B5045232).

Availability of data and materials

The data will be available if needed.

Declarations

Ethics approval and consent to participate
Not applicable.

Consent for publication
All authors agree to publish this manuscript in this journal.

Competing interests
The authors declare that there is no conflict of interest.

Author details
[1]Department of Pharmaceutical Engineering, Catholic University of Daegu, Hayang-Ro 13-13, Gyeongbuk, Gyeongsan City 38430, Republic of Korea. [2]College of Pharmacy, Ajou University, Suwon City 443-749, Korea.

Received: 8 September 2021 Accepted: 2 February 2022
Published online: 09 March 2022

References

Cho Y-D, Park Y-J (2010) Preparation and evaluation of novel fenofibrate-loaded self-microemulsifying drug delivery system (SMEDDS). J Pharm Investig 40(6):339–345
Cho Y-D, Park Y-J (2014) In vitro and in vivo evaluation of a self-microemulsifying drug delivery system for the poorly soluble drug fenofibrate. Arch Pharmacal Res 37(2):193–203
Choi YH, Han H-K (2018) Nanomedicines: current status and future perspectives in aspect of drug delivery and pharmacokinetics. J Pharm Investig 48(1):43–60
Danafar H et al (2018) Polylactide/poly (ethylene glycol)/polylactide triblock copolymer micelles as carrier for delivery of hydrophilic and hydrophobic drugs: a comparison study. J Pharm Investig 48(3):381–391
Fang J et al (2011) The EPR effect: unique features of tumor blood vessels for drug delivery, factors involved, and limitations and augmentation of the effect. Adv Drug Deliv Rev 63(3):136–151
Gupta B et al (2017) Solid matrix-based lipid nanoplatforms as carriers for combinational therapeutics in cancer. J Pharm Investig 47(6):461–473
Jin S-E et al (2018) Evaluation of nitroglycerin and cyclosporin A sorption to polyvinylchloride-and non-polyvinylchloride-based tubes in administration sets. J Pharm Investig 48(6):665–672
Karbownik MS, Nowak JZ (2013) Hyaluronan: towards novel anti-cancer therapeutics. Pharmacol Rep 65(5):1056–1074
Kim HS, Lee DY (2017) Photothermal therapy with gold nanoparticles as an anticancer medication. J Pharm Investig 47(1):19–26
Kim J-E, Park Y-J (2017a) High paclitaxel-loaded and tumor cell-targeting hyaluronan-coated nanoemulsions. Colloids Surf B 150:362–372
Kim J-E, Park Y-J (2017b) Improved antitumor efficacy of hyaluronic acid-complexed paclitaxel nanoemulsions in treating non-small cell lung cancer. Biomol Ther 25(4):411
Kim J-E, Park Y-J (2017c) Paclitaxel-loaded hyaluronan solid nanoemulsions for enhanced treatment efficacy in ovarian cancer. Int J Nanomed 12:645
Kim CH et al (2017) Surface modification of lipid-based nanocarriers for cancer cell-specific drug targeting. J Pharm Investig 47(3):203–227
Kirtane AR et al (2017) Polymer-surfactant nanoparticles for improving oral bioavailability of doxorubicin. J Pharm Investig 47(1):65–73
Kogan G et al (2007) Hyaluronic acid: a natural biopolymer with a broad range of biomedical and industrial applications. Biotech Lett 29(1):17–25
Leung EL-H et al (2010) Non-small cell lung cancer cells expressing CD44 are enriched for stem cell-like properties. PLoS ONE 5(11):e14062
Liang J et al (2016) Hyaluronan as a therapeutic target in human diseases. Adv Drug Deliv Rev 97:186–203
Liebmann J et al (1993) Cremophor EL, solvent for paclitaxel, and toxicity. Lancet 342(8884):1428
Maeda H et al (2013) The EPR effect for macromolecular drug delivery to solid tumors: improvement of tumor uptake, lowering of systemic toxicity, and distinct tumor imaging in vivo. Adv Drug Deliv Rev 65(1):71–79
Mercê ALR et al (2002) Aqueous and solid complexes of iron (III) with hyaluronic acid: potentiometric titrations and infrared spectroscopy studies. J Inorg Biochem 89(3–4):212–218
Mohtashamian S, Boddohi S (2017) Nanostructured polysaccharide-based carriers for antimicrobial peptide delivery. J Pharm Investig 47(2):85–94
Park O et al (2017) Recent studies on micro-/nano-sized biomaterials for cancer immunotherapy. J Pharm Investig 47(1):11–18
Sarisozen C et al (2017) Polymers in the co-delivery of siRNA and anticancer drugs to treat multidrug-resistant tumors. J Pharm Investig 47(1):37–49
Seo J et al (2018) Enhanced topical delivery of fish scale collagen employing negatively surface-modified nanoliposome. J Pharm Investig 48(3):243–250
Son G-H et al (2017) Mechanisms of drug release from advanced drug formulations such as polymeric-based drug-delivery systems and lipid nanoparticles. J Pharm Investig 47(4):287–296
Taurin S et al (2012) Anticancer nanomedicine and tumor vascular permeability; where is the missing link? J Control Release 164(3):265–275
Yang XY et al (2013) Hyaluronic acid-coated nanostructured lipid carriers for targeting paclitaxel to cancer. Cancer Lett 334(2):338–345

Zhao P et al (2012) Paclitaxel loaded folic acid targeted nanoparticles of mixed lipid-shell and polymer-core: in vitro and in vivo evaluation. Eur J Pharm Biopharm 81(2):248–256
Zhu M et al (2013) In situ structural characterization of ferric iron dimers in aqueous solutions: Identification of μ-oxo species. Inorg Chem 52(12):6788–6797

Publisher's Note